Supplementary Material

This Supplementary Material provides additional analyses supporting the manuscript "*Assessment of Snow Depth Retrievability from Passive Microwave Observations over Arctic Sea Ice: A Global Sensitivity Analysis.*" It is intended to complement the main content by expanding on the sensitivity analysis results and the assessment of the retrievable space for snow depth. To further substantiate the key conclusions of the manuscript, we perform correlation analyses using multi-year in-situ snow depth measurements in conjunction with AMSR2 observations. These supplementary results aim to verify whether the relationships inferred from the SMRT-based simulations and EFAST sensitivity analysis are consistently reflected in observational evidence across a broader range of environmental conditions.

In addition, because the 23.8 GHz, 36.5 GHz, and 89.0 GHz channels can be substantially influenced by atmospheric variability, we apply an atmospheric radiative transfer model to estimate and reduce atmospheric contributions as much as possible. This processing step is used to better isolate snow signals in the observed TBs, thereby enabling a more defensible comparison with the atmosphere-free forward simulations presented in the main manuscript.

1. Atmosphere correction on AMSR2 TBs

We corrected AMSR2 observed TBs using the Wentz model (Wentz and Meissner, 2000; Lu et al. 2022). The atmosphere correction accounts for seven parameters: wind speed, atmospheric water vapor, cloud liquid water, sea surface temperature, ice surface temperature, sea ice concentration, and multi-year ice concentration. The first five parameters are taken from the ERA5 reanalysis (Hersbach et al), while sea ice concentration (Spreen et al. 2008) and multi-year ice concentration (Ye and Heygster, 2015) are obtained from the University of Bremen.

2. Comparison with in-situ snow depth measurements

We used in situ observations from Snow and Ice Mass Balance Array (SIMBA) buoys deployed during 2012–2016 (Locations see Fig.S1) to evaluate the different GR algorithm (Preußer et al. 2025). Specifically, the buoy-measured snow depth records were matched to AMSR2 observations (within 6.25 km, 3 hours), and the corresponding TBs were extracted both from the original AMSR2 L1R product and from the

atmospherically corrected result. We further filtered the in situ snow depth measurements by selecting “pure ice” surface using a sea ice concentration threshold of SIC > 95%. All collocated observations had a MYIC greater than 20%.

Under this constraint, we evaluated four GRs:

1) GR(18/6)
2) GR(36/18)
3) GR(23/6)
4) GR(89/36)

In addition, we introduced an ERA5 snowfall dataset (Hersbach et al) to identify fresh snow conditions. If snowfall occurred on all the three days preceding a given in-suit measurement, we classified that measurement as a fresh snow measurement.

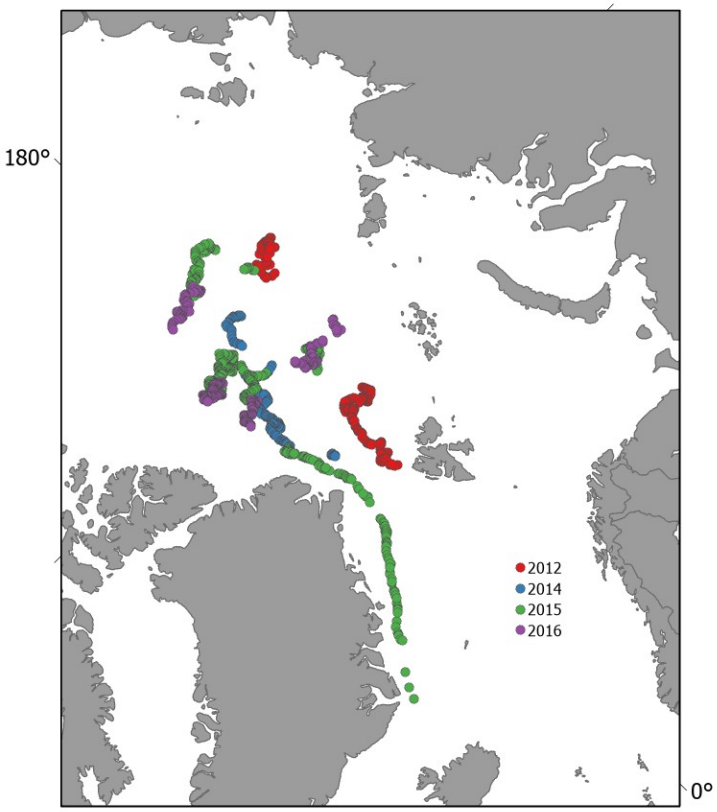

Fig.S1 SIMBA snow depth in-suit measurement locations

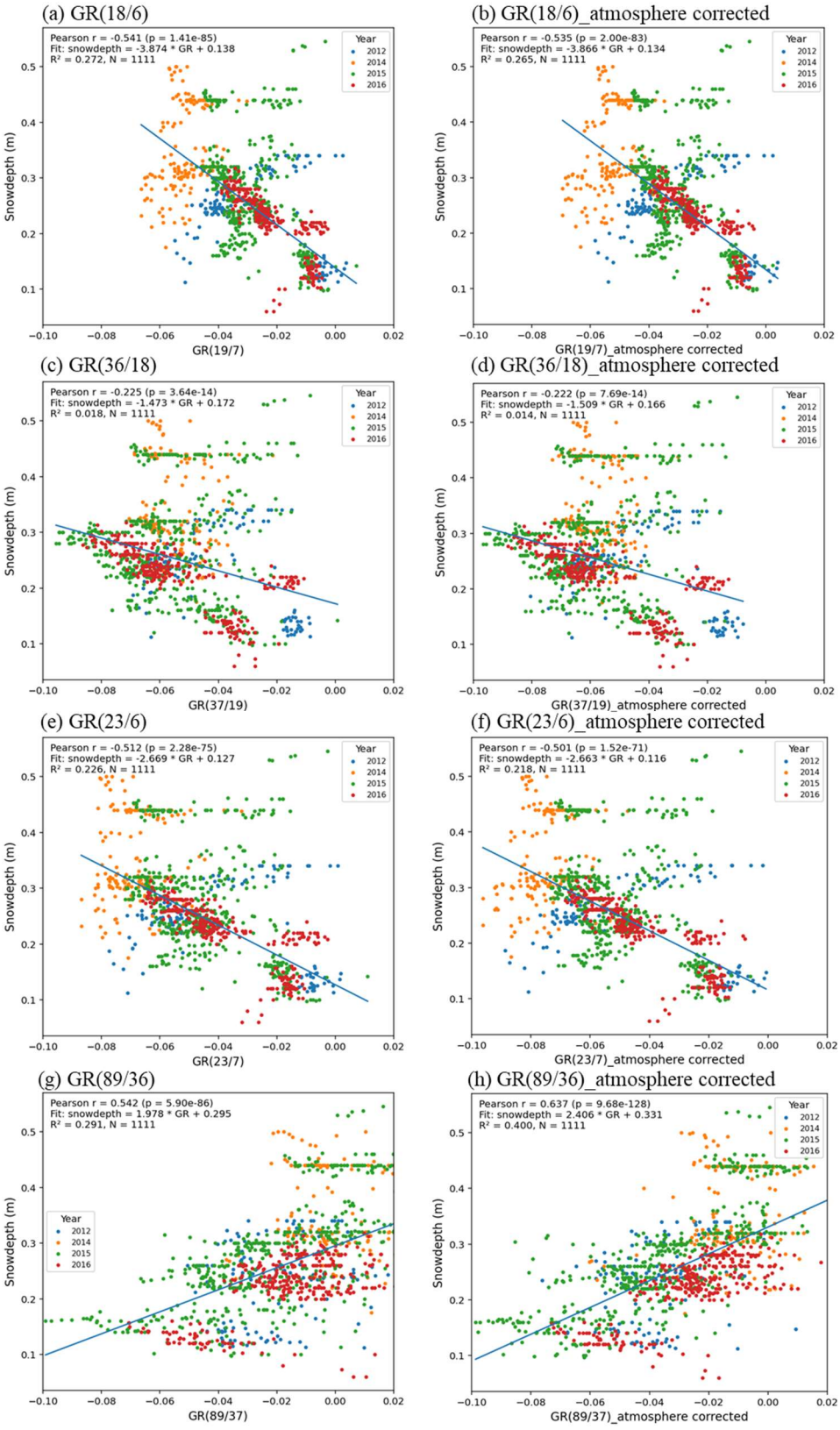

Fig.S2 Relationships between SIMBA snow depth and AMSR2 GR using original and atmospherically corrected TBs. Points are colored by year, solid lines denote linear fits, annotations report Pearson's *r*, *p*-value, and R^2 for each GR.

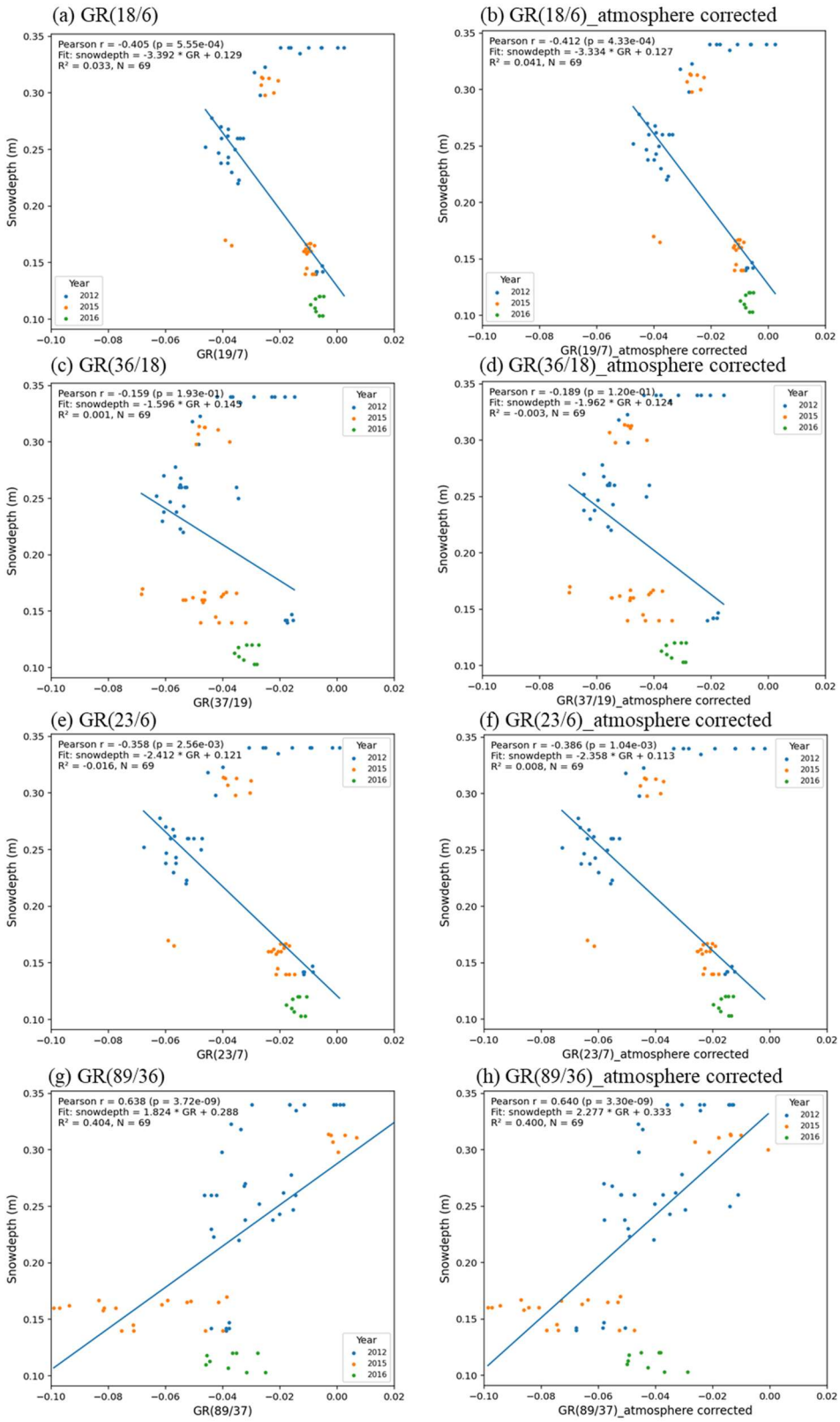

Fig.S3 Relationships between SIMBA snow depth and AMSR2 GR using original and atmospherically corrected TBs **during fresh snow measurement**. Points are colored by year, solid lines denote linear fits, annotations report Pearson's *r*, *p*-value, and R^2 for each GR.

As shown in Fig. S2, GR(89/36) exhibits the strongest correlation with the buoy-measured snow depth, followed by GR(18/6) and GR(23/6). For most GRs, the correlation changes only marginally after atmospheric correction. In contrast, GR(89/36) shows a pronounced improvement after correction, with the correlation increasing by nearly 0.1, far exceeding the changes observed for the other GR combinations.

Further, Fig. S3 indicates that GR(89/36) maintains consistently high performance under fresh snow conditions, with correlation values remaining stable at approximately 0.63–0.64. By comparison, the other GR algorithms exhibit a marked decrease in correlation for fresh snow.

Ref.

Wentz, F. J. and Meissner, T.: AMSR ocean algorithm, Algorithm Theoretical Basis Document (ATBD), Version 2, CA, USA, 2000.

Spreen, G. L., Kaleschke, L., and Heygster, G.: Sea ice remote sensing using AMSR-E 89-GHz channels, Journal of Geophysical Research: Oceans, 113, C02S03, https://doi.org/10.1029/2005JC003384, 2008.

Hersbach, H., Bell, B., Berrisford, P., Biavati, G., Horányi, A., Muñoz Sabater, J., Nicolas, J., Peubey, C., Radu, R., Rozum, I., Schepers, D., Simmons, A., Soci, C., Dee, D., and Thépaut, J.-N.: ERA5 hourly data on single levels from 1979 to present, Copernicus Climate Change Service (C3S) Climate Data Store (CDS) [data set], https://doi.org/10.24381/cds.adbb2d47, 2018.

Lu, J., Scarlat, R., Heygster, G., and Spreen, G.: Reducing weather influences on an 89 GHz sea ice concentration algorithm in the Arctic using retrievals from an optimal estimation method, Journal of Geophysical Research: Oceans, 127, e2019JC015912, https://doi.org/10.1029/2019JC015912, 2022.

Preußer, A., Nicolaus, M., and Hoppmann, M.: Snow depth, sea ice thickness and interface temperatures derived from measurements of SIMBA buoys deployed in the Arctic Ocean and Southern Ocean between 2012 and 2023, PANGAEA [data set], https://doi.org/10.1594/PANGAEA.973193, 2025.

Ye, Y. and Heygster, G.: Arctic multiyear ice concentration retrieval from SSM/I data using the NASA Team algorithm with dynamic tie points, in: Towards an Interdisciplinary Approach in Earth System Science, Springer, Cham, 99–108,

https://doi.org/10.1007/978-3-319-13865-7_12, 2015.